

Analysis of Air Distribution in a Double Tube Model Heat Exchanger System using Computational Fluid Dynamic (CFD)

Reniana¹✉, Darma¹, Paulus Payung¹

¹ Jurusan Teknik Pertanian dan Biosistem, Fakultas Teknologi Pertanian, Universitas Papua, Manokwari, INDONESIA.

Article History:

Received : 30 November 2023

Revised : 06 February 2024

Accepted : 07 March 2024

Keywords:

CFD,
Design,
Double-Tube,
Heat Exchanger,
Simulation.

Corresponding Author:

✉ ana.iner@gmail.com
(Reniana)

ABSTRACT

The double-tube model heat exchanger has a construction of three tube cylinders arranged into one. This model of heat exchanger has a fairly simple construction, making it easier to manufacture and speeding up the manufacturing process. Computational Fluid Dynamics (CFD) is software that can be used to optimize the design and performance evaluation process as well as to speed up the process and minimize costs in tool development because it can represent phenomena that occur in a system. This research aims to analyze air distribution in a double tube model heat exchanger system using CFD analysis and to validate the analysis results with experiments. Based on the research results, a double tube model heat exchanger has been created with an average performance of output temperature and air velocity reaching 97.8°C and 10.4 m/s at a coconut shell fuel consumption of 0.24 kg/minute. The results of evaluating experimental data with simulations obtained RMSE values between 59.33 – 71.69, and MAPE values between 26.26 – 32.93. Meanwhile, the results of the Paired Sample T-Test show that there is no real difference between experimental data and simulation data with an R-value of 0.875 – 0.964. CFD analysis in this research can be used as a reference in the optimization process and development of heat exchangers, especially double-tube models.

1. INTRODUCTION

A heat exchanger is a device used to facilitate the transfer of heat from a hot fluid to a cold fluid, which then becomes hot due to the heat exchange occurring within the system. According to Azwinur & Zulkifli (2019), the use of heat exchangers in the field of drying has become essential to address the issues of long drying times and the large areas required for drying. In drying equipment, heat exchangers play a crucial role, particularly in providing heat sourced from biomass combustion. These heat exchangers supply clean hot air free from smoke produced by biomass combustion, which can contaminate and lower the quality of the dried products. Currently, the most commonly used and developed type of heat exchanger is the shell and tube heat exchanger, as developed and evaluated by Fattah & Iskandar (2020); Aprianto *et al.* (2021); Ratnawati & Salim (2018); Jumianto (2023); Marawijaya *et al.* (2019), and Pasaribu *et al.* (2023). Overall, the performance and efficiency of these developments have shown satisfactory results. According to Setiorini & Faputri (2023), one reason for the popularity of this type of heat exchanger is its large surface area, which allows for optimal heat transfer and its compact shape and volume. However, one drawback of this type of heat exchanger is the complexity of its fabrication, as it consists mainly of small pipes arranged inside a cylindrical tube. Therefore, a simpler and easier-to-fabricate heat exchanger model is needed. One such model is the double-tube heat exchanger, which consists of three cylindrical tubes arranged into one unit. This model has a simpler construction, making it easier and faster to fabricate. Additionally, to optimize the design and performance evaluation

process, and to minimize costs, a tool is needed to represent the system within the designed device. According to [Arora \(2004\)](#), a tool or system is considered acceptable if it is cost-effective, efficient, practical, reliable, and durable. Computational Fluid Dynamics (CFD) is one such software tool that can be used to analyze phenomena occurring within a system. According to [Tuakia \(2008\)](#), CFD is a tool for predicting what will happen to a device or system under one or more boundary conditions. Applying CFD in system design, particularly in heat exchanger development, offers significant benefits as it can predict the phenomena occurring within the system. The application of CFD can speed up the process and reduce costs in designing or developing a system or device.

[Reniana et al. \(2017\)](#) conducted a study on aeration analysis in grain storage using silos with CFD. The analysis results showed satisfactory outcomes, with an average error between simulation and experiment ranging from 3.6% to 5.47%. [Jading et al. \(2017; 2018\)](#) performed CFD analysis on cyclones and pneumatic dryers, with an average error range of 0.10% to 4.594%. Additionally, [Baskara \(2023\)](#) designed a heat exchanger using CFD analysis. The study's results indicated that CFD analysis could increase the device's effectiveness from 34% to 39%. The purpose of this study is to analyze the air distribution in a double-tube heat exchanger system and validate the CFD analysis results with experimental data.

2. MATERIALS AND METHODS

The materials used in this study for constructing the double-tube heat exchanger unit include 2 mm thick stainless steel plates, 5 cm x 5 cm angle iron with 5 mm thickness, an 8-inch centrifugal blower (3-phase, 3 hp), coconut shells for biomass furnace fuel, and other supporting materials for constructing the heat exchanger. The tools used include a computer equipped with Ansys Fluent 2022 R1 software, 12-channel thermocouples, 4-channel thermocouples, anemometers, tachometers, stopwatches, a biomass furnace, and various workshop tools supporting the heat exchanger construction. Results of the Combine Harvester innovation are visible to others or adopters, measured by scores and categorized into three: difficult, moderately easy, and easy.

2.1. Research Procedure

This research consists of three main stages:

1. Design and Prototyping of the Double-Tube Heat Exchanger.

This stage begins with designing/drawing the heat exchanger to be made, as shown in Figure 1. The double-tube heat exchanger has a cylindrical shape. The unit is generally divided into several parts: the heating tube, middle tube, outer tube, hot (fire) inlet channel, air inlet channel, heat outlet channel, and air outlet channel. The unit is 122 cm long, with heating, middle, and outer tube diameters of 30 cm, 50 cm, and 70 cm, respectively. The diameters of the hot inlet, air inlet, heat outlet, and air outlet channels are 30 cm, 3 cm, 10 cm, and 20 cm, respectively. In this heat exchanger, a suction blower is placed at the end of the air outlet channel to draw air into the system through the air inlet channel. This blower rotates at 2800 rpm and is driven by a 6.5 HP engine.

2. Testing of the Double-Tube Heat Exchanger:

The testing is conducted by introducing heat (fire) generated from burning coconut shells using a biomass furnace into the hot inlet channel. Thermocouples are placed at 19 points within the heat exchanger for temperature measurement (Figure 1). Temperature data is collected every two minutes until the coconut shell burning process is complete. The obtained temperature data will be used for validation with CFD analysis results. The temperature data used for validation includes four measurement times. The input temperatures measured during the experiment for each measurement time are used as boundary conditions for the CFD simulation. The respective input air temperatures for simulations 1, 2, 3, and 4 are 419°C, 493°C, 680°C, and 728°C.

3. Simulation Using CFD:

The CFD simulation consists of three stages: preprocessing, processing, and postprocessing. The preprocessing stage involves building and analyzing a model using CFD. This includes creating the geometry of the heat exchanger and performing meshing with the default settings in Ansys Fluent 2022 R1. Boundary conditions for the model are then defined:

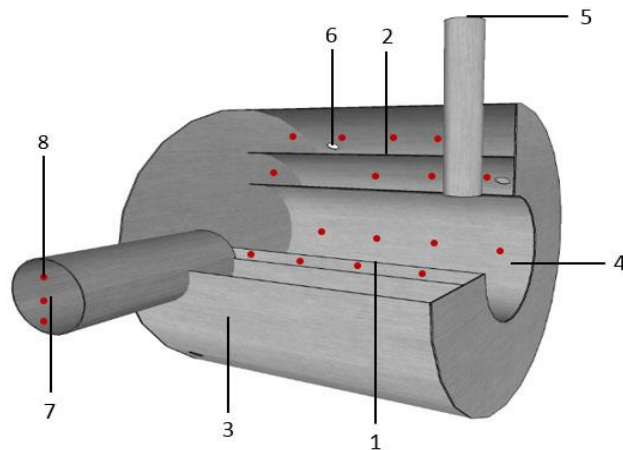


Figure 1. Design of the double-tube heat exchanger prototype: (1) Heating tube, (2) Middle tube, (3) Outer tube, (4) Hot (fire) inlet channel, (5) Heat outlet channel, (6) Air inlet channel, (7) Air outlet channel, (8) Temperature measurement points (red dots)

- a) Heat inlet: defines the surface for the hot inlet channel.
- b) Heat outlet: defines the surface for the hot outlet channel.
- c) Air inlet: defines the surface for the air inlet channel.
- d) Air outlet: defines the surface for the air outlet channel.
- e) Heat exchanger wall: defines the surface of the heat exchanger wall.
- f) Heat exchanger interior: defines the volume of the heat exchanger interior.

Each boundary condition definition is conducted according to the experimental conditions, including the input heat temperature and hot air velocity, the material properties of air and the heat exchanger wall (stainless steel). The default settings in Ansys Fluent 2022 R1 are used for conditions outside these parameters. The assumed value for the input air velocity is determined through trial and error until the output air velocity value approaches the experimental value of 10 m/s. Based on the trial and error results, with the input air velocity values ranging between 20 – 40 m/s, an input air velocity of 40 m/s is selected for the simulation process. The hot air input velocity is set according to the experimental conditions, which is 10 m/s. The measured input temperatures during the experiment for each measurement time are used as boundary conditions for the CFD simulation. Consequently, the input air temperature values for simulations 1, 2, 3, and 4 are 419°C, 493°C, 680°C, and 728°C, respectively.

The next step is the setup process with Energy – On and Viscous – Realizable $k-\epsilon$, standard wall settings. The processing stage involves iteratively calculating the input data using the equations involved until the smallest error is reached, using the default settings in Ansys Fluent 2022 R1. The post processing stage is the final step, where the CFD analysis results are interpreted in the form of images, graphs, and animations. At this stage, qualitative temperature data is collected at coordinates corresponding to the experimental measurement positions.

2.2. Data Validation

The purpose of data validation is to compare nineteen measured data points with the temperatures obtained from CFD analysis. The data validation includes calculating the Root Mean Square Error (RMSE), Mean Absolute Percentage Error (MAE), Pearson Correlation (R), and Paired Sample T-Test. The temperature data to be validated are four temperature data points taken simultaneously from the measurement points during experiment and simulation results.

3. RESULTS AND DISCUSSION

3.1. Air Temperature Distribution in the Heat Exchanger

The performance testing of the fabricated heat exchanger was conducted by introducing heat (fire) from the

combustion of coconut shells using a biomass burner into the heat inlet channel (Figure 2). Based on the test results, the average output temperature of the heat exchanger reached 97.8°C (ranging from 65.6°C to 140.3°C) with an average output air speed of 10.4 m/s over a processing time of 36 minutes with a coconut shell fuel consumption of 0.24 kg/min . For the purpose of connecting this heat exchanger to a Pneumatic Conveying Ring Dryer (PCRD), the temperature produced by this device is still relatively high, reaching up to 140.3°C with an average of 97.8°C . This high temperature is a concern as it may cause damage to the materials being dried, particularly for flour or starch products. Jading *et al.* (2021) reported that the temperature range for PCRD dryers is $50\text{--}100^{\circ}\text{C}$ at air speeds between $15\text{--}31\text{ m/s}$. Tethool *et al.* (2017) reported that the gelatinization temperature of natural sago starch is 73.2°C , and it will decrease if the starch is modified. Therefore, to utilize this heat exchanger connected to a PCRD dryer, temperature reduction and air speed increase are necessary. According to Jading *et al.* (2021), in PCRD drying, the contact time of the material with the drying air is shorter at higher air speeds, which accelerates the evaporation process and affects the quality of the resulting sago starch.



Figure 2. Testing the heat exchanger with the heat input source from coconut shell combustion: (a) biomass burner, (b) heat exchanger unit, (c) suction blower, (d) air intake channels (top, bottom, right, and left sides).

3.2. CFD Analysis Results

CFD analysis was performed four times with boundary conditions matching the experimental conditions. The input air temperature for simulations 1, 2, 3, and 4 were 419°C , 493°C , 680°C , and 728°C respectively. The input hot air speed and air speed for each simulation were the same, 10 m/s and 40 m/s respectively. Based on the results of simulations 1, 2, 3, and 4, the temperature ranges inside the heat exchanger were $23.6\text{--}394.5^{\circ}\text{C}$, $24.4\text{--}464.8^{\circ}\text{C}$, $25.7\text{--}680.1^{\circ}\text{C}$, and $26.6\text{--}726.8^{\circ}\text{C}$ respectively. Meanwhile, experimental results (Figure 3) showed temperature ranges inside the heat exchanger of $46.7\text{--}419.4^{\circ}\text{C}$, $49.5\text{--}493.8^{\circ}\text{C}$, $38\text{--}815.3^{\circ}\text{C}$, and $40.4\text{--}820.7^{\circ}\text{C}$ respectively. Figures 4 and 5 show the air velocity streamlines and temperature contours from the CFD simulation analysis.

Figure 4 shows that the temperature distribution inside the central part of the heat exchanger from the simulation results has an orange to red color gradient. This is because this part is the heating tube, which has a high temperature range in simulations 1, 2, 3, and 4: $340.5\text{--}394^{\circ}\text{C}$, $400.4\text{--}464.8^{\circ}\text{C}$, $581.5\text{--}680.1^{\circ}\text{C}$, and $622.2\text{--}726.8^{\circ}\text{C}$ respectively. Additionally, hot air circulates back after reaching the end of the closed tube to exit through the heat outlet channel (Figure 5). This condition causes the temperature to remain relatively stable, thus maintaining high temperatures in that part. However, the color contour from the CFD analysis shows a light blue to light green gradient between the heating tube and the central tube and between the central tube and the outer tube. This phenomenon occurs due to the heat transfer process from the exchanger walls to the incoming cold air, which increases in temperature as a result of conduction heat transfer through the exchanger tube walls and convection by the air itself. This condition was also observed during the experiment, where the cold air temperature increased after entering the heat exchanger. Ndeo *et al.* (2021) found similar results in their study using CFD simulation for air temperature inside a coffee drying house, showing uneven temperature distribution with varying color gradients. Similarly, Reniana *et al.* (2017) reported that

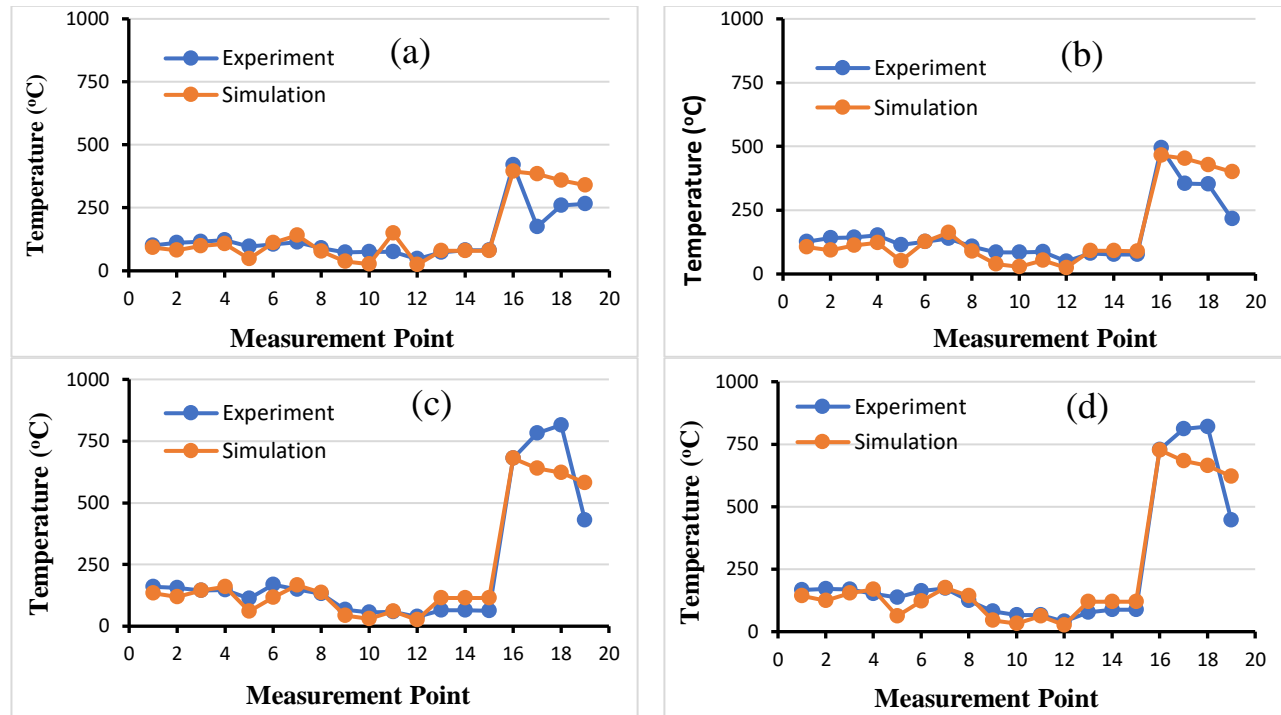


Figure 3. Air temperature distribution resulted from CFD simulation as compared to experiment measurement at different input temperatures: (a) 419 °C, (b) 493 °C, (c) 680 °C, (d) 728 °C.

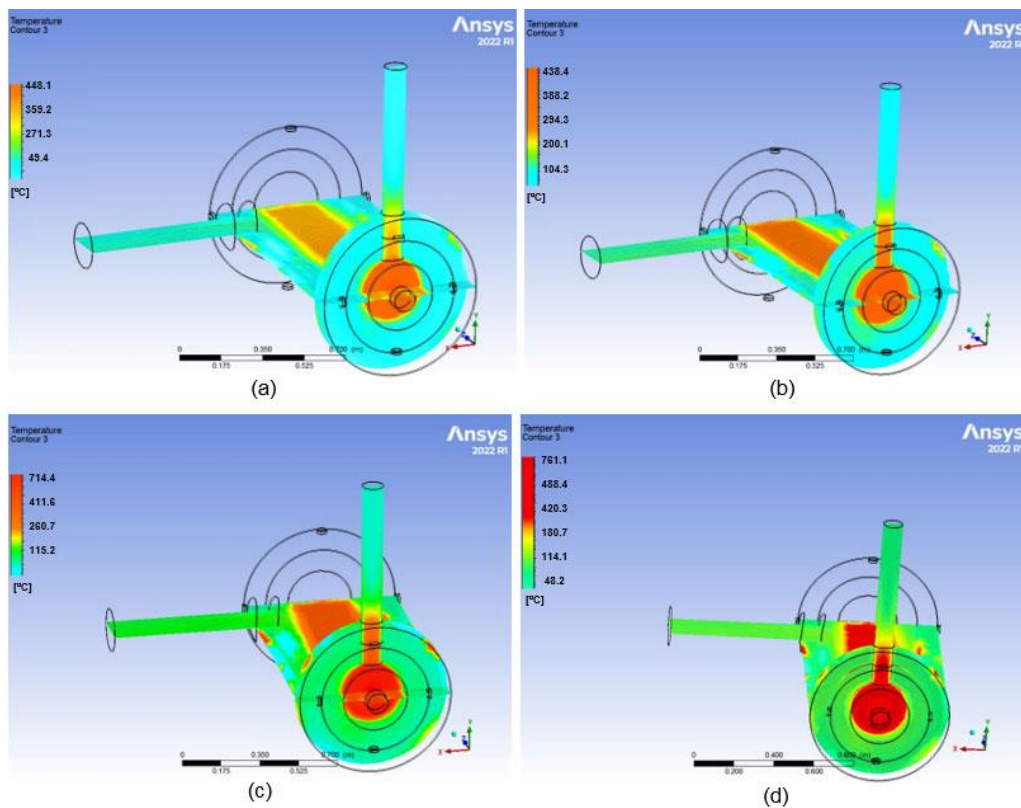


Figure 4. Air temperature distribution contours in the heat exchanger from CFD simulation with different input temperatures: (a) 419 °C, (b) 493 °C, (c) 680 °C, and (d) 728 °C.

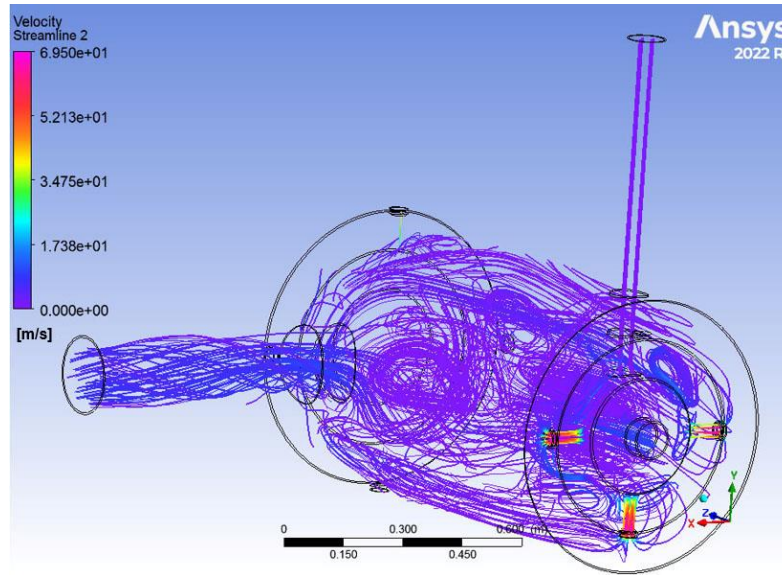


Figure 5. Air velocity streamline from CFD simulation.

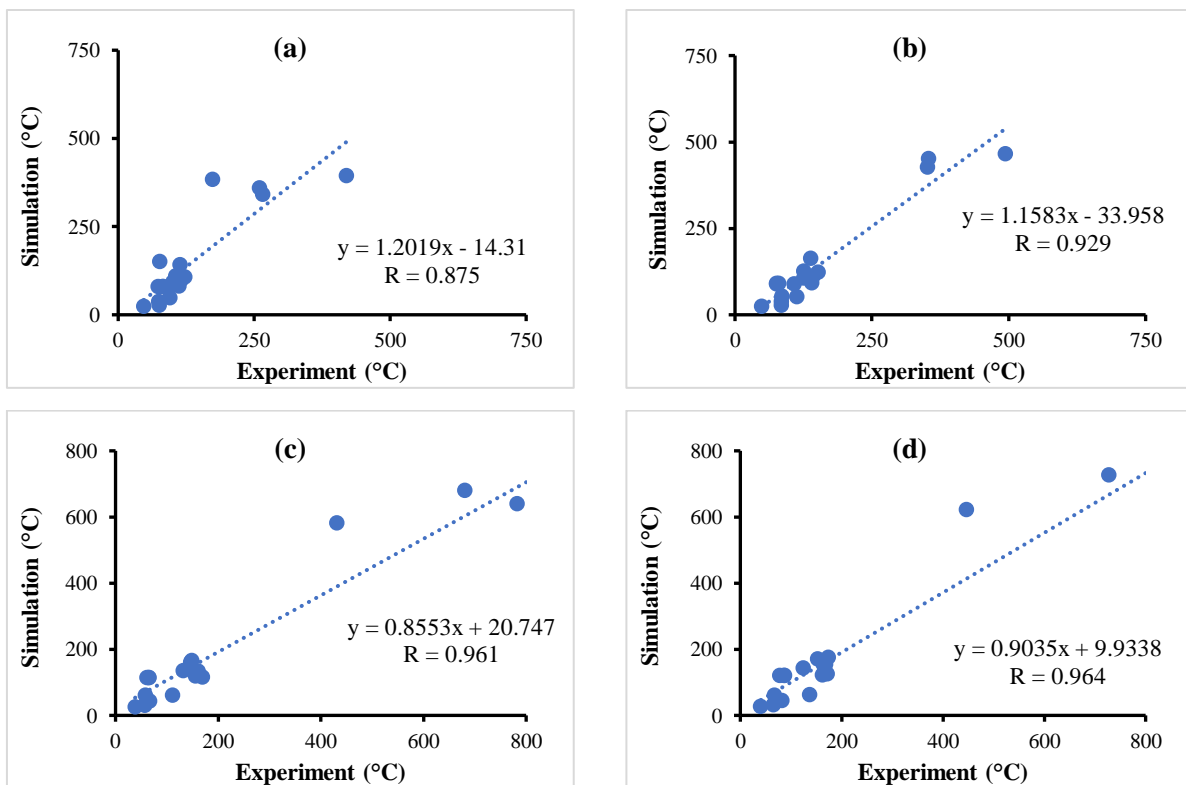


Figure 6. Relationship of experimental and CFD simulation temperatures with (a) 419 °C, (b) 493 °C, (c) 680 °C, and (d) 728 °C.

air temperature distribution in grain storage silos analyzed with CFD showed increasing temperatures closer to the outer silo walls. Rosyadi *et al.* (2017) also found uneven temperature distribution in a pneumatic conveyor dryer CFD simulation, with changes occurring when varying the input air speed.

3.3. Validation

Validation was conducted by comparing the temperature data from the CFD analysis with the air temperature data measured inside the heat exchanger at the same points/coordinates. Figure 6 shows the graph of the relationship between the experimental temperature and the CFD simulation temperature. The data validation in this study includes the calculation of Root Mean Square Error (RMSE), Mean Absolute Percentage Error (MAPE), Pearson Correlation (R), and Paired Sample T-Test. Tables 1 and 2 present the results of the validation of experimental data with CFD analysis.

Table 1. Results of evaluating experimental temperature data with CFD simulation.

Parameter	Input Temperature 419°C	Input Temperature 493°C	Input Temperature 680°C	Input Temperature 728°C	Average
RMSE	62.79	59.33	71.69	68.35	65.54
MAE	32.93	30.65	30.25	26.26	30.02
Correlation (R)	0.875	0.929	0.961	0.964	0.932

Table 2. Results of Paired Sample T-Test evaluation of experimental temperature data with CFD simulation.

Parameter	Input Temperature 419°C	Input Temperature 493°C	Input Temperature 680°C	Input Temperature 728°C
Average Experiment	130.66	158.13	225.47	240.74
Average Simulation	142.74	158.83	213.58	227.43
Std. Dev. Experiment	91.20	117.07	253.34	258.03
Std. Dev. Simulation	125.24	151.51	225.56	241.85
Sig.	0.417	0.961	0.485	0.411

Based on Table 1, the evaluation of experimental temperature data with simulation data yielded average RMSE, MAPE, and correlation (R) values of 65.54, 30.02, and 0.932, respectively. The RMSE values obtained in this study are relatively high, likely due to the CFD analysis not fully replicating the boundary conditions of the experiment, thus affecting the analysis results. One factor is the inlet air speed. In this study, the inlet air speed was determined through trial and error using CFD, ranging from 20-40 m/s, to achieve an outlet air speed close to the experimental value of 10 m/s. An inlet air speed of 40 m/s was used in this study. Additionally, the suction blower at the end of the air outlet channel was not defined in the CFD analysis to simplify and speed up the model creation process. The average MAPE obtained in this study ranged from 20-50%, specifically 30.02%, indicating that the model is still feasible for use. Other evaluation results show that the experimental data has a high correlation, with R values ranging from 0.875 to 0.964, indicating that more than 87% of the experimental temperature distribution can explain the simulation temperature distribution. The Paired Sample T-Test results for the four sets of experimental and CFD simulation temperature data showed no significant differences, with Sig. values greater than 0.05. This lack of significant difference indicates that the simulation data can represent the experimental data. Thus, the CFD analysis in this study can be used as a reference for optimizing and developing double-tube heat exchanger models.

The study by [Al-Kindi *et al.* \(2015\)](#) using CFD simulation on a rack-type dryer achieved R^2 values ranging from 0.8122 to 0.9209. [Jading *et al.* \(2018\)](#) reported that the validation of CFD simulation results on a pneumatic conveying ring dryer for sago had error values ranging from 0.1 to 2.04%. [Anisum *et al.* \(2016\)](#) reported that the CFD simulation results in a mushroom house had error values ranging from 0.7 to 2.62%.

In this study, the quality of the CFD simulation results is significantly influenced by the boundary conditions used in the analysis process, including input and output conditions, material properties, and the equations used. From the study results, optimization and development of the double-tube heat exchanger model can be carried out. One approach is to increase the diameter of the air inlet, which is expected to lower the outlet air temperature from the heat exchanger. Additionally, increasing the diameter of the air inlet can increase the inlet air speed, reducing the hot air contact time with the material, thereby minimizing quality degradation of the material due to high temperatures during

drying. After performing simulations by changing boundary conditions to achieve the desired simulation outputs, fabrication can proceed according to the design from the simulations. This approach can reduce time, effort, and costs in equipment development.

4. CONCLUSION

Based on the research results, a double-tube heat exchanger model was created, achieving an average output temperature of 97.8 °C (ranging from 65.6 °C to 140.3 °C) and an average output air speed of 10.4 m/s with a coconut shell fuel consumption of 0.24 kg/min. The evaluation of experimental data with simulation data yielded RMSE values ranging from 59.33 to 71.69, MAPE values ranging from 26.26 to 32.93. The Paired Sample T-Test results showed no significant differences between the experimental and simulation data, with R values ranging from 0.875 to 0.964. Further research is needed to improve the quality of CFD analysis, such as defining the suction blower as a rotating medium/object.

ACKNOWLEDGMENTS

We express our gratitude to the National Research and Innovation Agency (BRIN) and the Education Fund Management Institution (LPDP) for the research funding through the 2023 Research and Innovation for Advanced Indonesia (RIIM) scheme Round 2. This paper is dedicated to the late Dr. Abadi Jading, S.Pd., MP, the primary initiator of this research.

REFERENCES

- Arora, J.S. (2004). *Introduction to Optimum Design*, 2nd Ed. New York: McGraw-Hill Book Company.
- Al-Kindi, H., Purwanto, Y.A., & Wulandani, D. (2015). Analisis CFD aliran udara panas pada pengering tipe rak dengan sumber energi gas buang. *Jurnal Keteknikaan Pertanian*, *3*(1), 9-16.
- Anisum, N., Bintoro, & Goenadi, S. (2016). Analisis distribusi suhu dan kelembaban udara dalam rumah jamur (kumbung) menggunakan computational fluid dynamics (CFD). *Agritech*, *36*(1), 64-70. <https://doi.org/10.22146/agritech.10686>.
- Aprianto, G.B. Septian, Rey, P.D., & Aziz, A. (2021). Desain dan fabrikasi alat penukar kalor (heat exchanger) tipe shell and tube. *Metrik Serial Teknologi dan Sains*, *2*(1), 22-32.
- Azwinur, A., & Zulkifli, Z. (2019). Kaji eksperimental pengaruh baffle pada alat penukar panas aliran searah dalam upaya optimasi sistem pengering. *Jurnal Mesin Teknologi (SINTEK Jurnal)*, *13*(1), 8-14. <https://doi.org/10.24853/sintek.13.1.8-14>
- Baskara, G.P. (2023). Perancangan alat penukar panas (APK) Tipe U dengan memanfaatkan panas gas buang menggunakan simulasi CFD. *Jurnal Ilmiah Wahana Pendidikan*, *9*(2), 197-206. <https://doi.org/10.5281/zenodo.7567530>
- Fattah, F., & Iskandar, A. (2020). Analisis kinerja heat exchanger type shell and tube berbahan tembaga aliran searah dan aliran berlawanan tanpa radiator. *Motor Bakar: Jurnal Teknik Mesin*, *4*(1), 1-6.
- Jading, A., Bintoro, N., Sutiarso, L., & Karyadi, J.K.W. (2017). Temperature distribution simulation and the analysis of cyclones performance on sago starch pneumatic conveying recirculated dryers. *Asian J. Sci. Res.*, *11*(1), 62-83. <http://dx.doi.org/10.3923/ajsr.2018.62.83>
- Jading, A., Bintoro, N., Sutiarso, L., & Karyadi, J.K.W. (2018). Temperature and air velocity simulation on sago starch pneumatic conveying recirculated dryer using ansys fluent. *Agritech*, *38*(1) 2018, 88-99. <https://doi.org/10.22146/agritech.18251>
- Jading, A., Payung, P., & Tethool, F.F. (2021). Uji kinerja dan kelayakan finansial pengering pati sago tipe pneumatic conveying ring dryer. *Jurnal Teknik Pertanian Lampung*, *10*(2), 228-238. <http://dx.doi.org/10.23960/jtep-l.v10i2.228-238>.
- Jumianto. (2023). Perencanaan alat penukar kalor shell dan tube proses penyerapan residu dan pelepasan uap dengan kapasitas 2.550.000 btu/jam. *Jurnal Persegi Bulat*, *1*(2), 7-16. <https://doi.org/10.36490/jurnalpersegiulat.v1i2.470>
- Marawijaya. Tahdid, G., Trisnaliani, L., & Purna, C. (2019). Prototype heat exchanger type shell and tube ditinjau dari variasi jarak baffle dan laju alir massa udara panas. *Jurnal Kinetika*, *10*(1), 18-23.
- Ndeo, Y.P, Koehuan, V.A., & Bunganaen, W. (2021). Simulasi computational fluid dynamic (CFD) rumah pengering kopi menggunakan plastik ultraviolet (UV) solar dryer. *LONTAR: Jurnal Teknik Mesin*, *8*(01), 11-20.

- Pasaribu, H, Lumbangaol, P., Siagian, H.S., Napitupulu, R.A.M., Siagian, P., & Setyawan, E.Y. (2023). Simulasi CFD distribusi temperatur pada pengering biji kopi dengan sistem konveksi paksa. *SPROCKET: Journal of Mechanical Engineering*, *5*(1), 14-24. <https://doi.org/10.36655/sprocket.v5i1.1214>
- Ratnawati, R., & Salim, A. (2018). Desain ulang alat penukar kalor tipe shell and tube dengan material tube carbon stell dan stainless stell 304. *TURBO : Jurnal Program Studi Teknik Mesin*, *7*(1), 74-80. <http://dx.doi.org/10.24127/trb.v7i1.712>
- Reniana, Bintoro, S., & Nugroho, J. (2017). Analisis sistem aerasi pada penyimpanan gabah dalam silo menggunakan computational fluid dynamics (CFD). *JTEP: Jurnal Keteknikan Pertanian*, *5*(2), 187-194.
- Rosyadi, I, Sudrajad, A., Satria, D., Yusuf, Y., & Wijaya, K.T. (2017). Analisa laju aliran fluida pada mesin pengering konveyor pneumatik dengan menggunakan simulasi CFD. *Flywheel: Jurnal Teknik Mesin Untirta*, *3*(2), 48-51.
- Setiorini, I.A., & Faputri, A.F. (2023). Evaluasi kinerja heat exchanger jenis kondensor 1110-C tipe shell and tube berdasarkan nilai fouling factor pada unit purifikasi di ammonia plant PT X. *Jurnal Teknik Patra Akademika*, *14*(1), 23-30. <https://doi.org/10.52506/jtpa.v14i01.188>
- Tethool, E.F., Jading, A., & Dewi, A.M. (2017). Pengaruh fotooksidasi UV-C terhadap sifat fisikokimia dan baking expansion pati sagu (*Metroxylon sago*). *Agrointek*, *11*(2), 45-52. <https://doi.org/10.21107/agrointek.v11i2.2917>
- Tuakia, F. (2008). *Dasar-Dasar CFD Menggunakan Fluent*. ISBN: 978-979-1153-21-8, Informatika, Bandung: 331 pp.